Cell, Vol. 94, 339–352, August 7, 1998, Copyright ©1998 by Cell Press

Differential Requirement for Caspase 9 in Apoptotic Pathways In Vivo

Razqallah Hakem,*† Anne Hakem,*†
Gordon S. Duncan,*† Jeffrey T. Henderson,‡
Minna Woo,*† Maria S. Soengas,§
Andrew Elia,*† José Luis de la Pompa,*†
David Kagi,*† Wilson Khoo,*†
Julia Potter,*† Ritsuko Yoshida,*†
Stephen A. Kaufman,‖ Scott W. Lowe,§
Josef M. Penninger,*† and Tak W. Mak*†#
*Amgen Institute
Toronto, Ontario M5G 2C1
Canada
†Ontario Cancer Institute
Departments of Medical Biophysics and Immunology
University of Toronto
Toronto, Ontario M5G 2C1
Canada
‡Samuel Lunenfeld Research Institute
Program in Molecular Biology and Cancer
Mount Sinai Hospital
Toronto, Ontario M5G 1X5
Canada
§Cold Spring Harbor Laboratory
Cold Spring Harbor
New York, New York 11724
‖Amgen Inc.
Thousand Oaks, California 91320-1789

Summary

Mutation of Caspase 9 (Casp9) results in embryonic lethality and defective brain development associated with decreased apoptosis. *Casp9* $^{-/-}$ embryonic stem cells and embryonic fibroblasts are resistant to several apoptotic stimuli, including UV and γ irradiation. *Casp9*$^{-/-}$ thymocytes are also resistant to dexamethasone- and γ irradiation–induced apoptosis, but are surprisingly sensitive to apoptosis induced by UV irradiation or anti-CD95. Resistance to apoptosis is accompanied by retention of the mitochondrial membrane potential in mutant cells. In addition, cytochrome c is translocated to the cytosol of *Casp9*$^{-/-}$ ES cells upon UV stimulation, suggesting that Casp9 acts downstream of cytochrome c. Caspase processing is inhibited in *Casp9*$^{-/-}$ ES cells but not in thymocytes or splenocytes. Comparison of the requirement for Casp9 and Casp3 in different apoptotic settings indicates the existence of at least four different apoptotic pathways in mammalian cells.

Introduction

Apoptosis, or programmed cell death (PCD), is an intricately regulated process (White, 1993; Green and Martin, 1995; Steller, 1995; Nagata, 1997). Genetic studies of apoptosis in *Caenorhabditis elegans* have identified *ced-3* and *ced-4* as proapoptotic genes and *ced-9* as an antiapoptotic gene (Hengartner, 1996). Several mammalian homologs of CED-3, CED-4, and CED-9 have been identified. Apaf1 is homologous to CED-4 (Zou et al., 1997); members of the Bcl2 family are homologous to CED-9 (Reed, 1994); and at least 11 mammalian cysteine proteases ("caspases") are homologous to CED-3 (Cohen, 1997). The caspases are present in cells as inactive proenzymes that are activated after their processing into two subunits in response to apoptotic stimulation (Salvesen and Dixit, 1997). Activated caspases cleave a variety of important cellular proteins, other caspases, and some Bcl2 family members, leading to an irreversible commitment to cell death (Cheng et al., 1997; Cohen, 1997; Clem et al., 1998).

There is recent evidence that caspase function may be modulated by physical interaction with Apaf1, cytochrome c (Apaf2), and Bcl2 family members (Zou et al., 1997; Hu et al., 1998; Pan et al., 1998). Caspase 9 (Casp9)/Apaf3, a 45 kDa protein "also known as ICE-LAP-6 or Mch6" (Duan et al., 1996; Srinivasula et al., 1996), forms a multiprotein complex containing Apaf1 and cytochrome c (Li et al., 1997b). It has been proposed that cytochrome c initiates apoptosis by inducing the formation of the Casp9/Apaf1 complex. Physical association of Casp9 and Apaf1 is mediated by the interaction of their respective caspase recruitment domain (CARD) (Li et al., 1997b). CARD is also found in other caspases with large prodomains, such as Casp4 and Casp8, which can associate with Apaf1 in mammalian cells (Hu et al., 1998). The antiapoptotic protein Bcl-X_L has also been shown to interact with Casp9 and Apaf1, resulting in the inhibition of Casp9 activation (Hu et al., 1998; Pan et al., 1998). The association of Casp9 with antiapoptotic as well as proapoptotic proteins suggests a major role for Casp9 in the control of apoptosis in vivo.

Since some caspases sequentially process and activate others, a model has been proposed in which some caspases (such as Casp8 and -9) act as initiator or signaling proteases, while others (such as Casp3 and -7) act as effectors of apoptosis (Cohen, 1997). *Casp3*$^{-/-}$ mice have revealed that Casp3 is required for PCD in the central nervous system (CNS) and also in other apoptotic settings (Kuida et al., 1996; Woo et al., 1998). Casp3 is also essential for the nuclear changes associated with apoptosis, including chromatin condensation (Woo et al., 1998).

To investigate the physiological function of Casp9, gene targeting was used to generate mutant cell lines and mice deficient for Casp9. We report that Casp9 deficiency leads to defective brain development and embryonic lethality. Embryonic stem cells (ES), as well as mouse embryonic fibroblasts (MEF), are resistant to UV and γ irradiation, as well as several other stimuli. Casp9–deficient thymocytes are resistant to dexamethasone and γ irradiation but are sensitive to UV irradiation and α-CD95 killing. Our results identify four distinct apoptotic pathways differentially utilized by various cell types in response to different apoptotic stimuli.

To whom correspondence should be addressed.

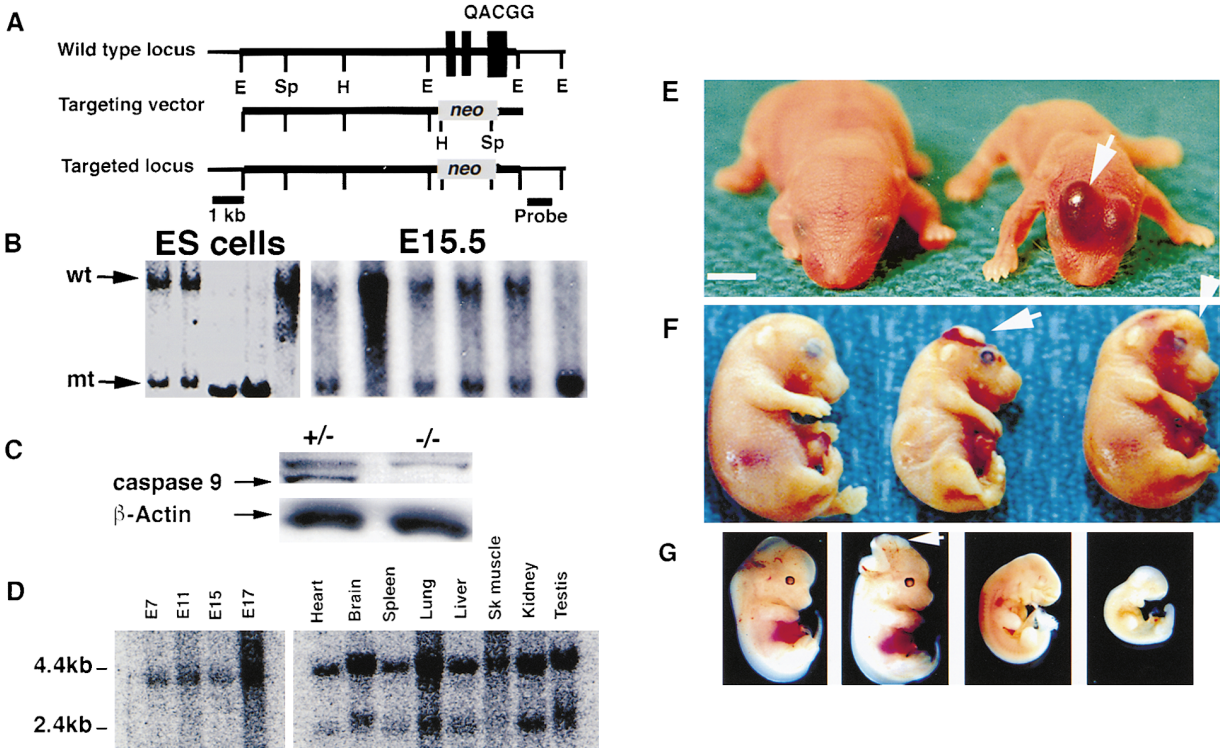

Figure 1. Gene Targeting of the Murine Casp9 Locus

(A) Restriction map of genomic *Casp9* sequences and the targeting vector. The *Casp9* exons replaced by neomycin in the targeted locus are shown as filled boxes. The *Casp9* flanking probe used for Southern blotting is indicated. E, EcoRI; H, HindIII; Sp, SpeI.

(B) Southern blot analysis of genomic DNA derived from wild-type, *Casp9*$^{+/-}$, and *Casp9*$^{-/-}$ ES cells (left panel) and E15.5 embryos (right panel). DNA was digested with SpeI and hybridized with the flanking probe. Arrows point to the 10.7 kb wild type (wt) and the 4.9 kb mutant (mt) bands.

(C) Western blot analysis of proteins extracted from *Casp9*$^{+/-}$ (+/−) and *Casp9*$^{-/-}$ (−/−) ES cells. Incubation with α-Casp9 antisera reveals the presence of the 45 kDa Casp9 protein in (+/−) ES cells but not in (−/−) ES cells.

(D) Northern blot analysis of total RNA extracted from E7, E11, E15, and E17 embryos and from different adult tissues. Hybridization was performed using ^{32}P-labeled *Casp9* cDNA.

(E) Examples of postnatal day 1 (pnd 1) wild-type (left) and *Casp9*$^{-/-}$ (right) mice. (F) E15.5 wild-type embryo (left) and two *Casp9*$^{-/-}$ mutant mice. (G) E12.5 wild-type embryo (left) and three *Casp9*$^{-/-}$ embryos showing the variable severity of the mutant phenotype. Arrows point to the characteristic perturbation of brain structure observed in the mutants. Bar represents 4 mm in (E), 3 mm in (F), and 600 μm in (G).

Results

Generation of *Caspase 9*$^{-/-}$ Mutant Mice

Casp9$^{+/-}$ ES cells were generated by homologous recombination, using a targeting vector designed to delete 2.6 kb of genomic DNA containing three coding exons of *Casp9*. This strategy led to the introduction of termination codons into all three reading frames and the removal of 138 amino acids, including the key pentapeptide QACGG, required for Casp9 activity (Duan et al., 1996) (Figure 1A). When the *Casp9* targeting construct was electroporated into ES cells, two G418-resistant colonies heterozygous at the *Casp9* locus were obtained (Figure 1B). These ES clones were used to generate chimeric mice, and both clones successfully contributed to germline transmission. Chimeras were backcrossed to C57BL/6J or CD1 mice, and *Casp9* heterozygotes were intercrossed to produce homozygous mutant offspring. The genotypes of the mice were confirmed by Southern blot analysis (Figure 1B). Homozygotes derived from both *Casp9*$^{+/-}$ clones had similar phenotypes in 129/C57BL/6 and 129/CD1 genetic backgrounds.

To study the effect of Casp9 deficiency on ES cell apoptosis, double knockout ES cell lines were generated by culturing *Casp9*$^{+/-}$ cells at an increased concentration of G418. *Casp9*$^{-/-}$ ES clones were obtained and confirmed by Southern blot and Western blot analyses (Figures 1B and 1C).

Caspase 9 Expression during Embryogenesis and in Adult Tissues

Northern blot analysis using a murine *Casp9* probe revealed the expression of a single *Casp9* transcript of about 4 kb in E7, E11, E15, and E17 embryos (Figure 1D). However, an additional 2.4 kb transcript, possibly the result of alternative splicing of the 4 kb *Casp9* transcript, was detected in adult tissues tested, including brain and spleen (Figure 1D). RT-PCR analysis was used to confirm the expression of *Casp9* in ES cells and thymocytes (data not shown). Thus, *Casp9* is expressed early in embryogenesis and ubiquitously in adult tissues.

Caspase 9 Mutation Results in Embryonic Lethality

Interbreeding of *Casp9*$^{+/-}$ mice showed that homozygosity for the *Casp9* mutation was lethal, since fewer

Table 1. Genotypic and Phenotypic Analysis of Newborn Mice and Embryos from *Caspase 9* Heterozygous Intercrosses

	Phenotype		Genotype			
Stage	Normal	Abnormal	*Casp9*$^{+/+}$	*Casp9*$^{+/-}$	*Casp9*$^{-/-}$	Total
Pnd 1	93	7	22	71	7	100
E15.5	23	8	6	17	8	31
E12.5	29	8	9	20	8	37
E10.5	13	0	3	7	3	13

Postnatal day 1 (pnd 1) mice and embryos were genotyped by PCR and Southern blot, as shown in Figure 1B. The embryos were collected on day 10.5, 12.5, and 15.5 of pregnancy from *Casp9*$^{+/-}$ females crossed to *Casp9*$^{+/-}$ heterozygous males. The abnormal phenotype of the newborn mice and embryos consisted in the perturbation of their brain structure and morphology, as shown in Figures 1E–1G. The mutant phenotype was similar in 129/C57BL/6 and 129/CD1 genetic backgrounds.

than 8% of postnatal day (pnd) 1 mice were homozygotes (Table 1). At birth, *Casp9*$^{-/-}$ mice were consistently smaller than control littermates, and most died before pnd 3 (Figure 1E). Timed matings indicated that the onset of abnormalities was at about E12.5 (Figure 1G). At E12.5 and E15.5, *Casp9*$^{-/-}$ mice displayed protrusions of the brain tissue from the skull (Figures 1F and 1G). These data show that Casp9 is required for embryonic and postnatal survival.

Caspase 9 Mutation Leads to a Defect in Cortex and Forebrain Structures

Casp9$^{-/-}$ newborn mice exhibited a striking perturbation in cortical morphology (Figures 2A and 2B), reminiscent of that observed in *Casp3*$^{-/-}$ mice (Kuida et al., 1996, and not shown). Examination of pnd 1 *Casp9*$^{-/-}$ animals revealed gross perturbations of brain structure that were most severe within the cortex and forebrain. Sites of ectopic cortical growth (Figure 2D, asterisk) and a lack of commissural structures were also frequently observed in these animals. *Casp9*$^{-/-}$ animals exhibited a significant expansion of their ventricular zone. In addition, there was a gross disorganization of ventricular structure, with the lateral ventricles frequently becoming contiguous with the subdural space through disruptions in the dorsal cortex (Figure 2D). Intracerebral hemorrhage in postnatal *Casp9*$^{-/-}$ animals was also a common finding. *Casp9*$^{-/-}$ animals also exhibited accumulations of necrotic and occasionally ectopic tissue outside the skull proper, particularly along the anterior aspect of the cerebral hemispheres (Figure 2B). Within these regions, the bone matrix was discontinuous and grew around these masses, suggesting that they occurred relatively early in the course of cranial development.

To understand the origin of the morphological disruptions observed in the *Casp9*$^{-/-}$ mutants, we examined PCD during the embryonic development of these animals. Examination of E12.5 embryos by TUNEL labeling demonstrated substantially less cell death within the developing CNS of *Casp9*$^{-/-}$ embryos compared to control littermates. As shown in Figures 2H and 2J, significant reductions in PCD were observed in the mutant in both the cerebral cortex and trigeminal ganglion at this stage. However, no difference in PCD was observed between *Casp9*$^{+/-}$ and *Casp9*$^{-/-}$ embryos at other sites such as brain-associated mesenchymal tissue (not shown). The number of BrdU-positive cells at E12.5 and E15.5 was also consistently increased over controls within the ventricular zone of *Casp9*$^{-/-}$ embryos (Figures 2K–2N, and not shown). Thus, Casp9, like Casp3, is required for PCD during brain development.

Impaired Apoptosis in *Caspase 9*$^{-/-}$ ES Cells in Response to a Wide Range of Apoptotic Stimuli

The effect of the Casp9 mutation on apoptosis was further accessed by comparative studies of two independent *Casp9*$^{-/-}$ ES cell clones, wild-type and *Casp3*$^{-/-}$ ES cell lines. *Casp9*$^{-/-}$ ES cells were resistant to all apoptotic stimuli tested, including adriamycin, UV and γ irradiation, etoposide, sorbitol, cisplatinum, and anisomycin (Figure 3A, and not shown). Analysis of apoptotic features of the rare *Casp9*$^{-/-}$ ES cells that died following UV irradiation showed the expected changes in phosphatidyl serine (PS) on the plasma membrane, as detected by Annexin V-FITC staining. However, like *Casp3*$^{-/-}$ ES cells, *Casp9*$^{-/-}$ ES cells that died following UV irradiation showed incomplete chromatin condensation, as judged by DAPI staining and electron microscopy (EM) (Figure 3B, and not shown).

Requirement of Caspase 9 in MEFs for PCD in Response to Some, but Not All, Apoptotic Stimuli

We next examined apoptosis in MEFs. *Casp9*$^{-/-}$ MEFs, like *Casp3*$^{-/-}$ MEFs, were resistant to apoptosis induced by UV and γ irradiation, adriamycin, and etoposide (Figure 3C, and not shown). To extend these analyses, MEFs were transformed with *E1A/ras* oncogenes to increase their sensitivity to several apoptotic stimuli, including γ irradiation, mTNF-α, and chemotherapeutic drugs. Transformed *Casp9*$^{-/-}$ MEFs remained resistant to adriamycin but underwent apoptosis in response to mouse TNF-α treatment (Figure 3D), showing normal apoptotic features including chromatin condensation and DNA degradation (Figure 3E, and not shown). Consistent with these data, *Casp9*$^{-/-}$ primary MEFs transiently transfected with a *TNF-R1* expression vector succumbed to apoptosis (Figure 3C). Furthermore, studies of *Casp9*$^{-/-}$ MEFs as target for cytotoxic T lymphocytes indicated that Casp9, like Casp3 (Woo et al., 1998), is not required for CTL target cell lysis mediated via the perforin/granzyme pathway (not shown).

To demonstrate that the apoptotic defects of the *Casp9*$^{-/-}$ MEFs were a direct consequence of Casp9 deficiency, a wild-type human *CASP9* gene was reintroduced into *E1A/ras* MEFs by retroviral gene transfer.

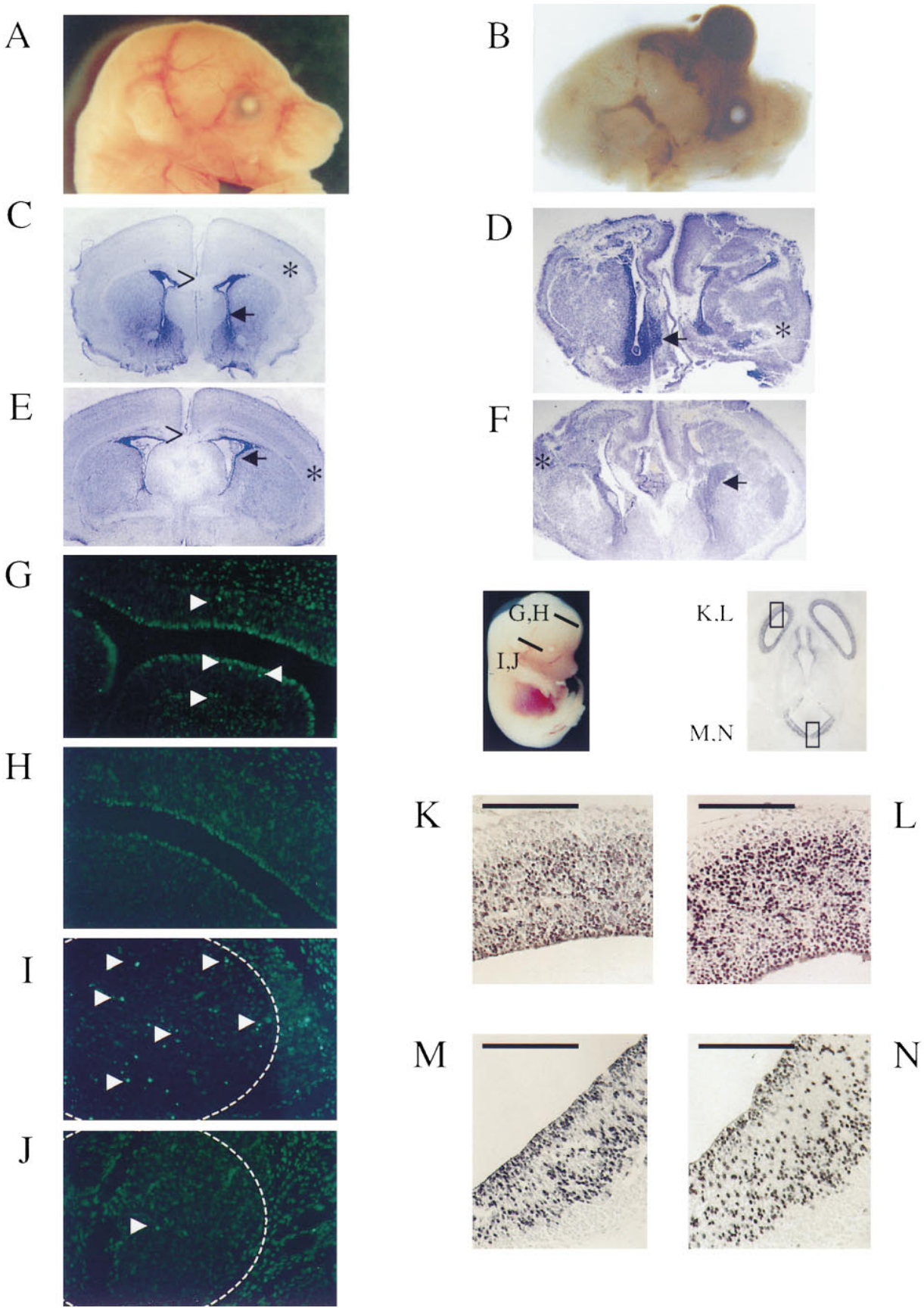
A
B
C
D
E
F
G
H
I
J
G,H
I,J
K,L
M,N
K
L
M
N

Upon treatment with adriamycin, *Casp9*$^{-/-}$ MEFs expressing exogenously transfected *Casp9* died at levels similar to wild-type controls (not shown).

These results demonstrate that, in MEFs, Casp9 is not necessary for the TNF-induced pathway of apoptosis, nor for CTL target cell lysis mediated via the perforin/granzyme pathway, but that apoptotic pathways induced by other stimuli require Casp9 expression.

Normal Development of Thymocytes and Lymphocytes in the Absence of Caspase 9

To determine the role of Casp9 during the development and PCD of thymocytes and lymphocytes, we analyzed these cells in *Casp9*$^{-/-}$ pnd 2 mice, as well as those in *Casp9*$^{-/-}$*; Rag2*$^{-/-}$ somatic chimeric mice. Thymocyte numbers were similar in *Casp9*$^{-/-}$ and *Casp9*$^{+/-}$ pnd 2 mice ($12.7 \times 10^6 \pm 2$ and $14.9 \times 10^6 \pm 1.6$, respectively; $n = 2$). Similarly, numbers of thymocytes obtained from 6-week-old *Casp9*$^{-/-}$*; Rag2*$^{-/-}$ and *Casp9*$^{+/-}$*; Rag2*$^{-/-}$ chimeric mice were comparable ($143 \times 10^6 \pm 84$ and $110 \times 10^6 \pm 65$, respectively; $n = 6$), as were numbers of splenocytes ($78 \times 10^6 \pm 15$ and $70.7 \times 10^6 \pm 19$, respectively; $n = 6$). However, lymph nodes (LN) of 6-week-old reconstituted *Casp9*$^{-/-}$*; Rag2*$^{-/-}$ chimeric mice were consistently enlarged compared to those in *Casp9*$^{+/-}$*; Rag2*$^{-/-}$ controls ($99.4 \times 10^6 \pm 10.4$ and $50.5 \times 10^6 \pm 9.7$, respectively; $n = 6$). Flow cytometric analysis showed no significant differences in the percentages of various thymocyte, splenocyte, and LN subpopulations present in *Casp9*$^{-/-}$ mice as compared with controls (not shown).

Requirement of Caspase 9 for Thymocyte Apoptosis in Response to γ Irradiation and Dexamethasone

Apoptosis was assayed in *Casp9*$^{-/-}$, *Casp3*$^{-/-}$, and wild-type thymocytes in response to a variety of apoptotic stimuli. *Casp9*$^{-/-}$ thymocytes, but not *Casp3*$^{-/-}$ or wild-type thymocytes, were resistant to apoptosis induced by dexamethasone or γ irradiation (Figure 4A). Furthermore, *Casp9*$^{-/-}$ thymocytes showed resistance to etoposide-induced PCD, but not to apoptosis induced by α-CD95, TNF-α, UV irradiation, heat shock, or sorbitol-induced osmotic shock (Figure 4A, and not shown). Those *Casp9*$^{-/-}$ thymocytes that did die after treatment with dexamethasone exhibited normal apoptotic features, including changes to PS on the plasma membrane and chromatin condensation (Figures 4A and 4D). These data demonstrate that Casp9 is required for thymocyte apoptosis in response to two major apoptotic stimuli, dexamethasone and γ irradiation.

Caspase 9 Is Required for Splenocyte Apoptosis in Response to γ Irradiation

Like *Casp9*$^{-/-}$ thymocytes, *Casp9*$^{-/-}$ splenocytes were resistant to γ irradiation (Figure 4B). However, Casp9 deficiency did not protect splenocytes from several other apoptotic stimuli, including UV irradiation, sorbitol-induced osmotic shock, and several chemotherapeutic drugs, such as adriamycin, etoposide, and cisplatinum (Figure 4B, and not shown). As shown in Figure 4B, Casp3 deficiency did not rescue splenocytes from PCD induced by UV or γ irradiation. However, we have previously shown that Casp3 is required for apoptotic morphological changes in lymphocytes following UV and γ irradiation (Woo et al., 1998).

Casp9–deficient splenocytes that did die in response to UV or γ irradiation showed normal PS plasma membrane changes but aberrant chromatin condensation, as assessed by DAPI staining (Figures 4B and 4E). Thus, Casp9 function is essential for the γ irradiation–induced cell death of splenocytes and the completion of chromatin condensation in response to a range of apoptotic signals, including UV and γ irradiation.

Caspase 9 and Apoptosis of Activated Splenocytes

The PCD of activated splenocytes lacking Casp9 was analyzed in response to α-CD95 or α-CD3ϵ antibodies. While activated *Casp3*$^{-/-}$ lymphocytes were resistant to PCD induced by these stimuli (Woo et al., 1998), dose–response and time course analysis indicated that *Casp9*$^{-/-}$ cells were completely sensitive to these stimuli and showed normal apoptotic features, including PS plasma membrane changes as well as chromatin condensation (Figures 4C and 4E, and not shown). Furthermore, activation-induced cell death (AICD) was not affected in the absence of Casp9 (not shown).

Thus, unlike Casp3, Casp9 is required for neither AICD nor for the α-CD3– or α-CD95–mediated apoptosis of activated splenocytes.

Caspase 9 Mutation Affects Mitochondrial Membrane Potential

Apoptosis is always accompanied by a decrease in mitochondrial membrane potential ($\Delta\psi m$) (Mignotte and Vayssiere, 1998). Flow cytometric determinations of $DiIC_1 5$ were used to visualize time courses of $\Delta\psi m$ changes in *Casp9*$^{+/-}$, *Casp3*$^{-/-}$, and *Casp9*$^{-/-}$ thymocytes treated with dexamethasone (Figure 5). Interestingly, untreated *Casp9*$^{-/-}$ thymocytes exhibited a lower $\Delta\psi m$ compared to untreated *Casp9*$^{+/-}$ and *Casp3*$^{-/-}$ cells, indicating a Casp9–dependent defect in the maintenance of $\Delta\psi m$ in these cells. When treated with dexamethasone, *Casp9*$^{+/-}$ and *Casp3*$^{-/-}$ thymocytes died

Figure 2. Morphology of *Caspase 9*$^{-/-}$ Mice

Overview of the cranium at pnd 1 of (A) *Casp9*$^{+/-}$ and (B) *Casp 9*$^{-/-}$ littermates. The overlying skin has been removed for clarity. (C–F) Thionin-stained coronal forebrain sections from pnd 1 mice viewed at several levels. (C) and (E), *Casp9*$^{+/-}$ mice; (D) and (F), *Casp9*$^{-/-}$ mice. Note the invasion of the cortical tissue (asterisks) and expansion of the ventricular zone (arrows) in *Casp9*$^{-/-}$ mice. The cortical disruption observed in *Casp9*$^{-/-}$ mice also typically resulted in a lack of commissural structures, such as the corpus callosum (open arrowheads, C and E). (G–J) TUNEL sections of (G and I) *Casp9*$^{+/-}$ and (H and J) *Casp 9*$^{-/-}$ littermates at E12.5. Relative levels of the horizontal forebrain sections (G and H) and trigeminal ganglion sections (I and J, dotted boundaries) are shown in the inset. At these sites, *Casp9*$^{-/-}$ embryos exhibit significantly fewer apoptotic nuclei (arrowheads) than their *Casp9*$^{+/-}$ littermates. (K–N) BrdU-labeled sections of (K and M) *Casp9*$^{+/-}$ and (L and N) *Casp9*$^{-/-}$ littermates at E12.5 (bars represent 150 μm). The relative position of micrographs within the horizontal plane is shown in the inset. At this age, increased BrdU-positive cells are observed in *Casp9*$^{-/-}$ mice compared to controls.

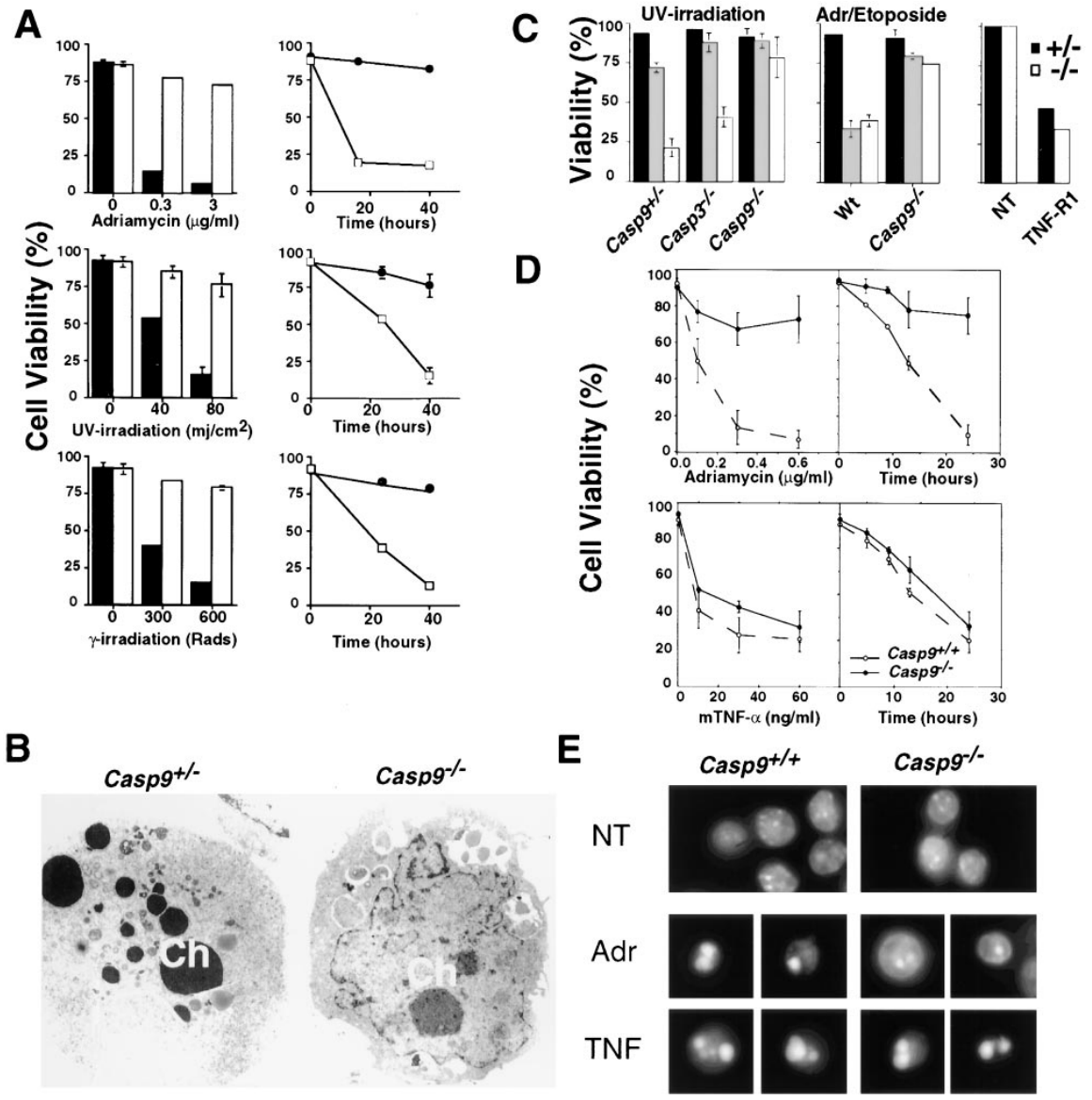

Figure 3. Impaired Apoptosis in *Caspase 9*$^{-/-}$ ES Cells and MEFs

(A) Induction of apoptosis of *Casp9*$^{-/-}$ and *Casp9*$^{+/-}$ cells in response to adriamycin, UV, or γ irradiation. Left panels: Cells were treated with various doses of the indicated stimuli and analyzed 40 hr later by Annexin V-FITC and PI costaining and flow cytometry. Solid bars, *Casp9*$^{+/-}$; open bars, *Casp9*$^{-/-}$. Right panels: *Casp9*$^{+/-}$ (squares) and *Casp9*$^{-/-}$ (circles) ES cells were treated with a single dose of adriamycin (0.3 μg/ml), UV irradiation (80 mJ/cm^2), or γ irradiation (600 rads) and analyzed at the indicated times by Annexin V and PI staining and flow cytometry.

(B) Electron microscopy of dead wild-type (left) and *Casp9*$^{-/-}$ (right) ES cells. Cells were treated with UV irradiation (80 mJ/cm^2) for 24 hr and processed for visualization by electron microscopy. Ch, chromatin.

(C) Induction of apoptosis of *Casp9*$^{-/-}$, *Casp3*$^{-/-}$, and *Casp9*$^{+/-}$ primary MEFs. Apoptosis was induced and cells were assayed at the indicated time points by Annexin V and PI staining and flow cytometry. Left panel: UV irradiation (40 mJ/cm^2). Solid bars, untreated (NT); gray bars, 24 hr after treatment; open bars, 48 hr after treatment. Middle panel: Adriamycin (0.3 μg/ml; 20 hr); Etoposide (100 μM; 20 hr). Solid bars, NT; gray bars, adriamycin (Adr) ; open bars, etoposide. Right panels: Cells were transiently transfected with a *GFP* expression vector only (NT), or in combination with a *TNF-R1* expression vector (TNF-R1). Twenty-four hours posttransfection, the % of viability (the ratio between the % of fluorescent cells in the analyzed culture compared to the % of fluorescent cells in the *GFP* transfected cultures) was determined. Results of a representative experiment are shown, n = 3. Solid bars, *Casp9*$^{+/-}$; open bars, *Casp9*$^{-/-}$.

(D) Cell death of *E1A/Ras*-transformed MEFs; *Casp9*$^{+/+}$ (empty circles) and *Casp9*$^{-/-}$ (filled circles/dashed lines). Transformed MEFs were treated with increasing amounts of adriamycin (left upper panel) or mTNF-α (left lower panel) and harvested 24 hr later. *E1A/Ras* MEFs were treated with a single dose of adriamycin (0.2 μg/ml; right upper panel) or mTNF-α (50 ng/ml; right lower panel) and collected at the indicated time points. Cell death was determined by trypan blue exclusion.

(E) Fluorescence microscopic visualization of DAPI staining of nuclear chromatin from wild-type and *Casp9*$^{-/-}$ transformed MEFs, either untreated (NT) and attached to the plate, or dead (floating) following 24 hr treatment with 0.2 μg/ml of adriamycin (Adr) or 50 ng/ml mTNF-α (TNF).

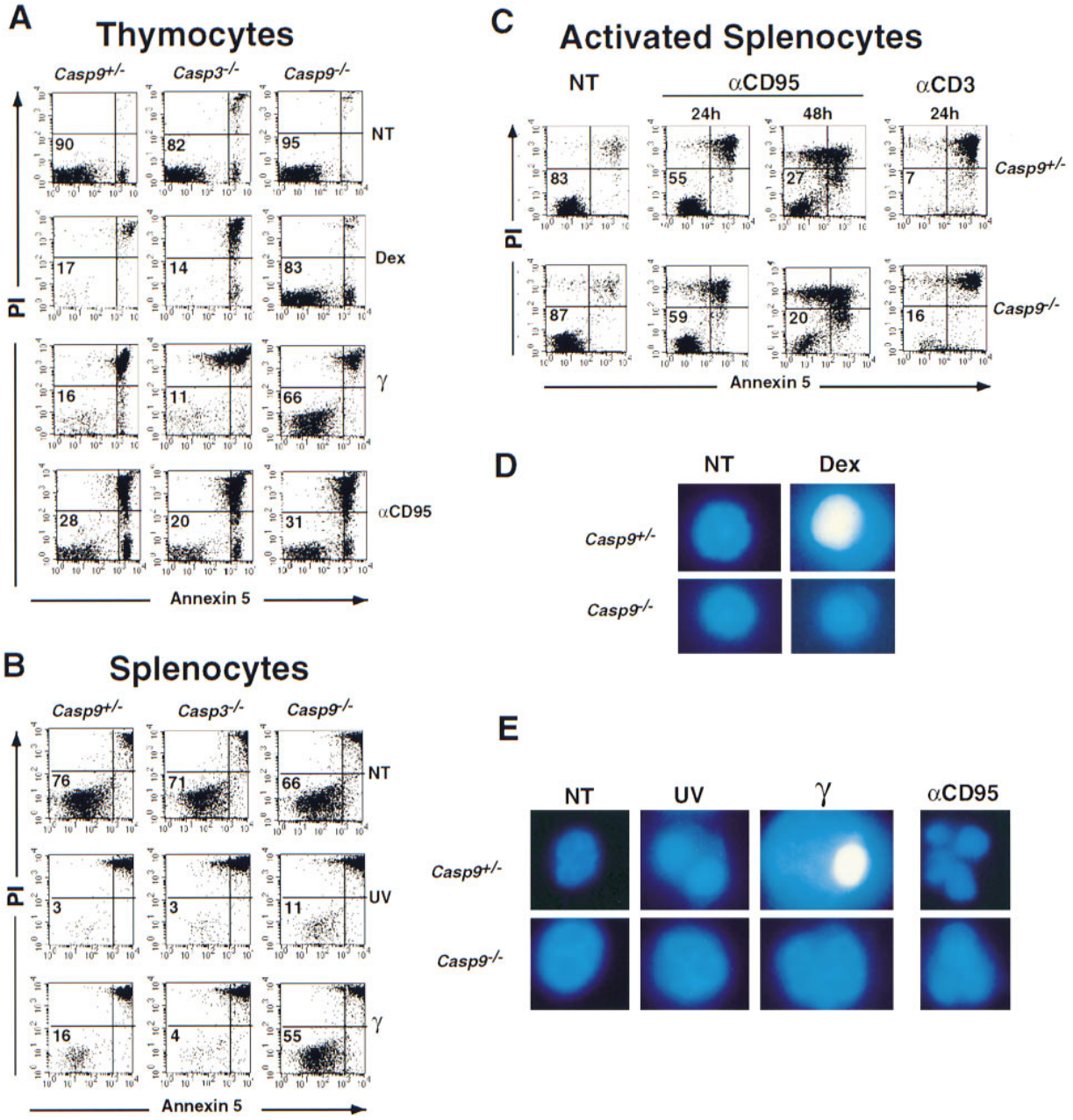

Figure 4. Requirement for Caspase 9 for Apoptosis of Thymocytes and Splenocytes in Response to Some, but Not All, Stimuli

(A–C) Fluorescence dot blots of Annexin V- and PI-stained thymocytes, naive or activated splenocytes from *Casp9*$^{+/-}$*; Rag2*$^{-/-}$ (*Casp9*$^{+/-}$), *Casp3*$^{-/-}$, or *Casp9*$^{-/-}$*; Rag2*$^{-/-}$ (*Casp9*$^{-/-}$) mice. Cells were either untreated (NT) or treated for 24 hr or 48 hr with dexamethasone (Dex, 1 μM), γ irradiation (γ, 600 rads), UV irradiation (UV, 40 mJ/cm^2), α-CD95 (1 μg/ml), or α-CD3 (1 μg/ml). The percentages of viable cells are indicated.

(D and E) Fluorescence microscopic visualization of DAPI staining of DNA from (D) *Casp9*$^{+/-}$ and *Casp9*$^{-/-}$ thymocytes and (E) splenocytes either untreated (NT) or treated with dexamethasone, UV, or γ irradiation. DAPI staining was also performed on activated splenocytes treated for 24 hr with α-CD95.

rapidly, and death was accompanied by a total loss of Δψm. However, *Casp9*$^{-/-}$ thymocytes treated with dexamethasone resisted further loss of Δψm and retained their (abnormally low) Δψm (Figure 5).

Thus, in addition to its function during thymocyte apoptosis in response to dexamethasone, Casp9 also plays a role in the regulation Δψm, both in resting thymocytes and in thymocytes responding to apoptotic stimuli.

Caspase 9 Acts Downstream of Mitochondrial Cytochrome c Release

Cytochrome c is required for PCD in vivo (Li et al., 1997a; Zhivotovsky et al., 1998) and for the activation of Casp9 and -3 in vitro (Kluck et al., 1997; Li et al., 1997b; Yang et al., 1997; Zou et al., 1997). The release of cytochrome c from the mitochondria during apoptosis precedes the changes of Δψm and caspase activation (Bossy et al.,

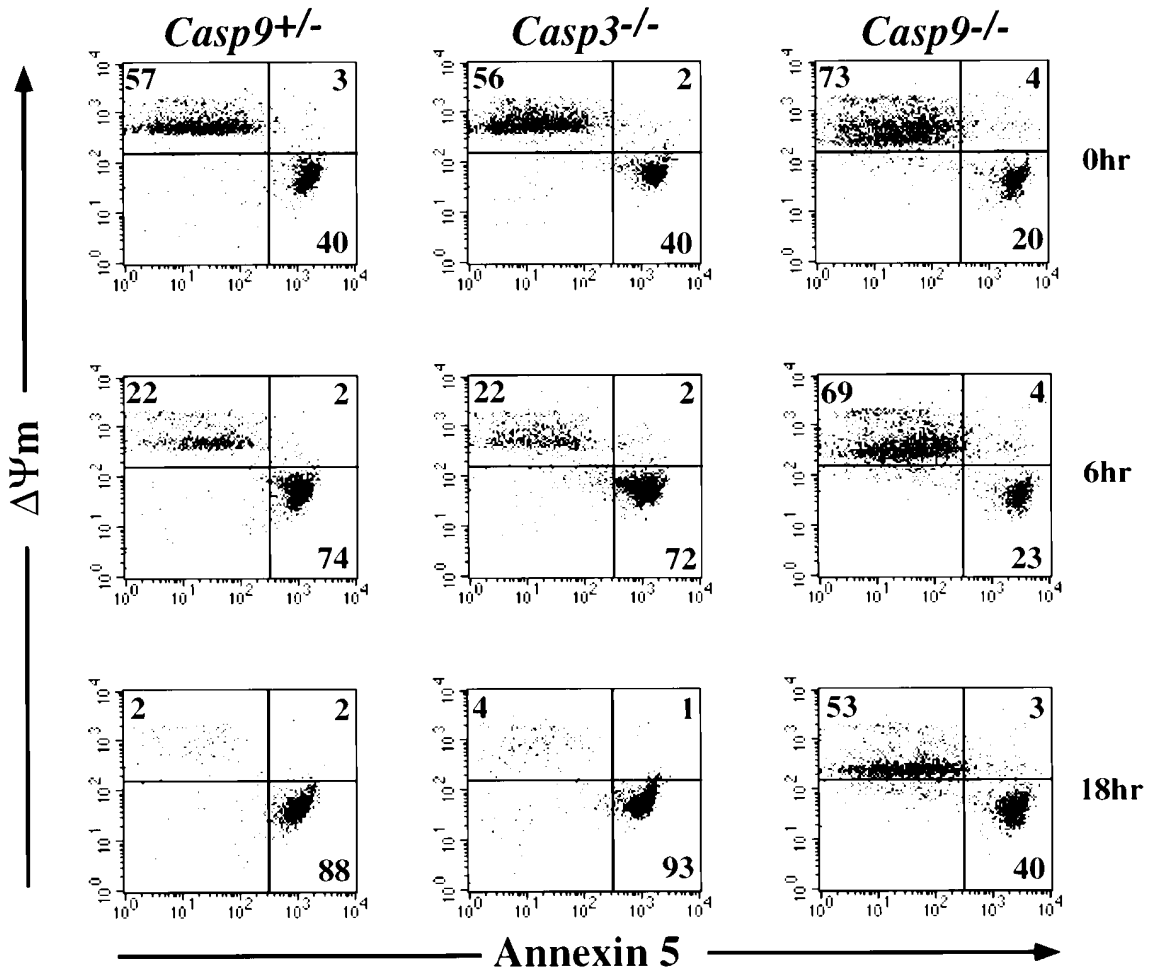

Figure 5. Mitochondrial Membrane Potential in the Absence of Caspase 9

Flow cytometric analysis of $\Delta\psi$m and Annexin V staining of *Casp9*$^{+/-}$*; Rag2*$^{-/-}$ (*Casp9*$^{+/-}$), *Casp3*$^{-/-}$, and *Casp9*$^{-/-}$*; Rag2*$^{-/-}$ (*Casp9*$^{-/-}$) thymocytes untreated (0 hr) or treated with 1 μM of dexamethasone for 6 or 18 hr. The percentages of the different populations stained positively for $\Delta\psi$m level and Annexin V are indicated.

1998). Furthermore, it has been shown that mitochondrial cytochrome c release, in response to apoptotic stimuli, is not affected by the pancaspase inhibitor peptide zVAD-fmk (Bossy et al., 1998) or by the apoptotic inhibitor viral protein p35 (Kharbanda et al., 1997).

The effect of Caspase 9 on cytochrome c release has been accessed using the *Casp9* mutant cells. Following UV irradiation, cytochrome c levels in the cytosol of both *Casp9*$^{-/-}$ and *Casp9*$^{+/-}$ ES cells were significantly increased compared to untreated controls, but not significantly different from each other (Figure 6A). Cytochrome c release from mitochondria in *Casp9*$^{-/-}$ ES cells and MEFs following UV stimulation was confirmed immunohistochemically, using an α-cytochrome c antibody (not shown). Therefore, cytochrome c translocation to the cytosol of these Casp9–deficient cells in response to UV irradiation is not sufficient to trigger their PCD. Thus, Casp9 acts downstream of mitochondrial cytochrome c release.

Caspase 9 Requirement for Caspase Activation In Vivo

Studies in vitro have suggested that Casp9 is the most upstream member of the apoptotic protease cascade that is triggered by the interaction of cytochrome c, Apaf1, and dATP (Li et al., 1997b). We investigated the role of Casp9 during the activation of the caspase cascade in a variety of cell types in response to several apoptotic stimuli. In ES cells, in which Casp9 deficiency resulted in resistance to all stimuli tested, there was a complete absence of procaspase processing (including pro-Casp3 and -8) following UV irradiation (Figure 6B, and not shown). The block in caspase processing was accompanied by a lack of cleavage of PARP, Rb, and the fluorogenic molecule AcDEVD-AMC, a substrate for Casp3 and Casp3-like caspases (Figure 6C, and not shown). Thus, in ES cells, Casp9 is required for the activation of the caspase cascade in response to UV irradiation.

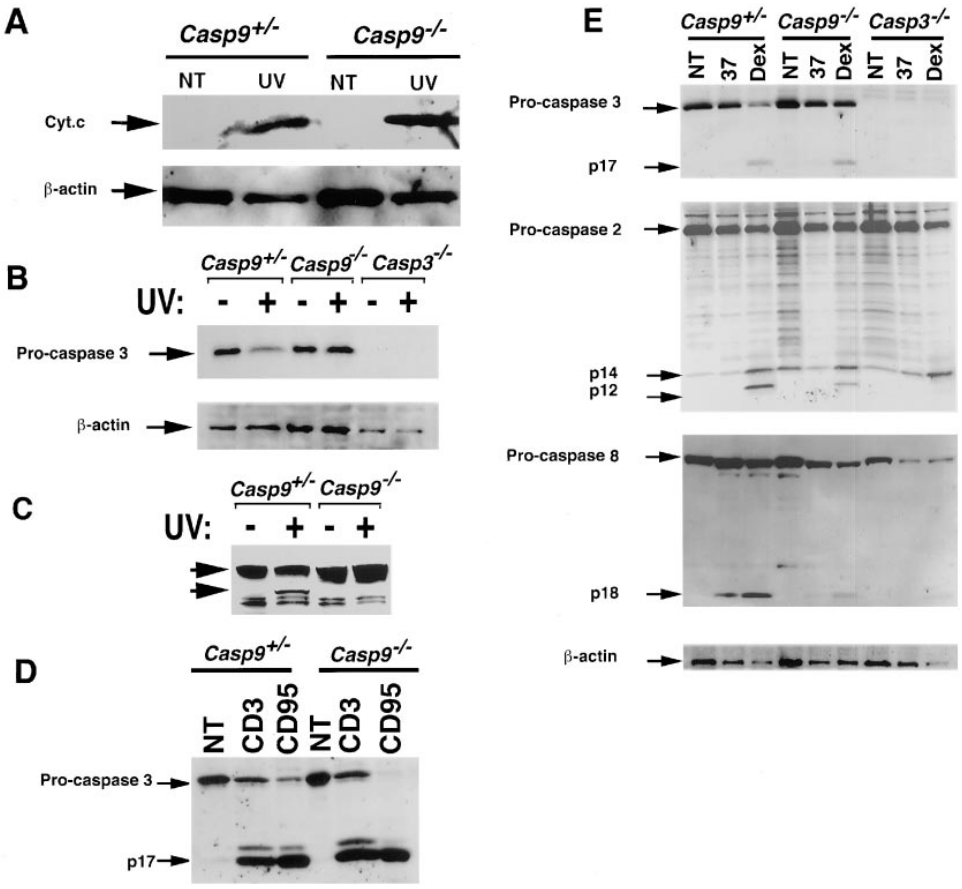

Figure 6. Cytochrome c Translocation to the Cytosol and Caspase Activation in *Casp9*$^{-/-}$ Cells

(A) Cytochrome c (Cyt.c) translocation to the cytoplasm in response to UV irradiation. *Casp9*$^{+/-}$ and *Casp9*$^{-/-}$ ES cells were treated with UV irradiation (80 mJ/cm^2) and cultured for an additional 6 hr. Cytosolic fractions were prepared from untreated (NT) and treated (UV) cells. Western blot analyses were performed using α-cytochrome c and anti-β-actin MAbs.

(B) Absence of Casp3 activation in *Casp9*$^{-/-}$ ES cells. Immunoblots of total proteins from *Casp9*$^{+/-}$, *Casp9*$^{-/-}$, and *Casp3*$^{-/-}$ ES cells 8 hr after UV irradiation (80 mJ/cm^2) were incubated with α-Casp3 and anti-β actin MAbs.

(C) Absence of PARP cleavage in *Casp9*$^{-/-}$ ES cells. Cells were treated as in (B), and PARP cleavage was assayed with an α-PARP MAb. The unprocessed form of PARP (113 kDa) as well as the 89 kDa processed form are indicated.

(D) Casp3 processing in activated T cells deficient for Casp9. Splenocytes were either untreated (NT) or activated and stimulated for 24 hr with α-CD3 (CD3) or α-CD95 (CD95) MAbs. Western blots were performed with an α-Casp3 MAb. Pro-Casp3 (32 kDa) and a processed form (p17) are indicated.

(E) Casp2, -3, -8, and β-actin in immunoblots of total proteins from *Casp9*$^{+/-}$, *Casp9*$^{-/-}$, and *Casp3*$^{-/-}$ thymocytes 8 hr after either no treatment (NT), incubation at 37°C (37), or treatment with 1 μM dexamethasone (Dex) at 37°C. Procaspases as well as their processed forms are indicated.

However, in activated *Casp9*$^{-/-}$ T cells stimulated with α-CD3ε or α-CD95, efficient processing of Casp3 and Casp8 occurred in both cases (Figure 6D, and not shown). In *Casp9*$^{-/-}$ thymocytes treated with dexamethasone, pro-Casp2, -3, -7, and -8 underwent processing to a limited extent (Figure 6E, and not shown). Cleavage of PARP and Rb was observed in dexamethasone-treated *Casp9*$^{-/-}$ thymocytes (not shown). These data indicate that Casp9 is differentially required in different cell types for caspase processing.

Discussion

Apoptosis is essential for normal development. Perturbations of the regulation or execution of developmental PCD usually result in profoundly detrimental effects. Emerging evidence indicates that these effects are cell type– and stimulus-specific.

Caspase 9 and Brain Development

The regulation of apoptosis is crucial for normal development of the CNS. Mutation of antiapoptotic Bcl2 family members, such as Bcl-X_L, triggers increased developmental apoptosis within the CNS, resulting in embryonic lethality at E13 (Motoyama et al., 1995). In null mutants of proapoptotic Bcl2 family members such as Bax, the survival of some neural cells is enhanced (Knudson et al., 1995; Deckwerth et al., 1996), resulting in a developmental increase in numbers of sympathetic and facial motor neurons in these animals. In addition, neurons from these animals are able to survive growth factor deprivation or axotomy-induced target deinnervation.

Caspase activation is known to be regulated by "inhibitor of apoptosis" proteins (IAPs), which inactivate some caspase family members through direct physical interaction via the BIR domain (Roy et al., 1997; Deveraux et al., 1998). In addition, high levels of some IAP family members, such as neural IAP (NIAP), have been shown to be principally confined to the nervous system neurons (Liston et al., 1996). Taken together, these features attest to the importance of PCD in regulating the development of the CNS.

In this study, we have demonstrated that the absence of Casp9 leads to a dramatic disturbance of telencephalic development that apparently results from decreased apoptosis in this region. A reduction in PCD could also account for the increased BrdU-positive cells observed within the germinal zones of *Casp9*$^{-/-}$ mutants, consistent with the survival of greater numbers of neuroepithelial progenitors. As a consequence, both the ventricular zone and forebrain cortical structures are expanded in these mutant mice, disrupting cortical organization and ultimately resulting in intracranial hemorrhage and death.

The gross morphological features observed in *Casp9*$^{-/-}$ mice are remarkably similar to those observed in mice lacking Casp3 (Kuida et al., 1996). Both mutants exhibit a profound disturbance of cortical morphology, an expanded germinal zone, and hydrocephaly, suggesting that these mutations affect a common cellular apoptotic pathway dependent on both Casp9 and Casp3.

Caspase 9 and Thymocyte Development

PCD is a critical process in thymocyte development. Several stimuli are known to induce thymocyte apoptosis, including glucocorticoids, CD95 ligation, and UV and γ irradiation. Overexpression of Bcl2 in thymocytes results in their resistance to apoptosis induced by dexamethasone, α-CD3, or γ irradiation, but not by α-CD95 (Sentman et al., 1991). Bcl2 has been shown to act at the mitochondrial level and upstream of Casp3 activation (Kluck et al., 1997; Yang et al., 1997). However, *Casp3*$^{-/-}$ thymocytes remain sensitive to several apoptotic stimuli, including dexamethasone and γ irradiation (Kuida et al., 1996; Woo et al., 1998), indicating that in thymocytes the antiapoptotic effect of Bcl2 is Casp3–independent.

The involvement of other caspases in thymocyte PCD has recently been documented. A study of *Casp2*$^{-/-}$ mice revealed that Casp2 is not important for thymocyte apoptosis (Bergeron et al., 1998). Casp11 has been shown to interact with Casp1 and to be essential for its activation (Wang et al., 1998). However, deficiency of either Casp1 or Casp11 in thymocytes results in partial resistance to α-CD95 killing, but not to other apoptotic stimuli (Kuida et al., 1995; Wang et al., 1998). In the present study, we show that, like Bcl2 overexpression, mutation of *Casp9* protects thymocytes from dexamethasone- and γ irradiation–induced cell death. Thus, we have identified Casp9 as essential for thymocyte PCD in response to dexamethasone and γ irradiation.

Caspase 9 and Apoptosis in Response to γ Irradiation

Defective apoptosis is a major factor in tumor formation (Thompson, 1995). Fusion of the *Bcl2* proto-oncogene to the immunoglobulin heavy chain locus occurs frequently in human follicular lymphomas (Bakhshi et al., 1985; Tsujimoto et al., 1985). In addition, several tumor suppressor genes and oncogenes are involved in the regulation of apoptosis. For example, p53 is required for cell death induced by different stimuli, including γ irradiation. A lack of p53 in thymocytes results in their resistance to ionizing irradiation-induced apoptosis (Lowe et al., 1993). Both homozygous and heterozygous *p53* mutant mice of advanced age develop a wide range of tumors, including thymomas (Donehower, 1996).

In this study, Casp9 deficiency protected thymocytes, splenocytes, MEFs, and ES cells from γ irradiation–induced cell death. *Casp9*$^{+/-}$ mice at 7 months of age were healthy, phenotypically normal, and did not show any sign of tumor formation. However, these mice may develop tumors as they age further. The fact that, like p53 deficiency, Casp9 deficiency results in resistance to apoptosis induced by γ irradiation or a variety of chemotherapeutic drugs suggests that Casp9 may play a role during tumor development or progression.

Caspase 9– and Caspase 3–Dependent Apoptotic Pathway

In vitro studies have previously identified Apaf1, cytochrome c, and Casp9 as participants in a complex important for Casp3 activation. In vitro depletion of Casp9 from cytosolic fractions resulted in the failure of Casp3 activation (Li et al., 1997b). These findings point to the existence of an apoptotic pathway dependent on both Casp9 and Casp3. The existence of such a pathway in vivo was confirmed in our study, since both *Casp9*$^{-/-}$ and *Casp3*$^{-/-}$ ES cells were resistant to several apoptotic signals, including UV irradiation. Those *Casp9*$^{-/-}$ ES cells that died in response to UV irradiation showed abnormal morphological features reminiscent of Casp3 deficiency (Woo et al., 1998). Furthermore, the lack of Casp9 in UV-irradiated ES cells resulted in a blockade of the processing of Casp3 as well as other caspases. This role of Casp9 in ES cells apparently cannot be assumed by other caspases, such as Casp8, even though Casp8 is expressed in ES cells and is capable of binding to Apaf1 (Hu et al., 1998, and not shown).

Thus, in ES cells, UV irradiation preferentially triggers the activation of an apoptotic pathway involving Casp9 and Casp3. Mutation of Casp9 or Casp3 produces similar effects on brain apoptosis and development, suggesting that the pathway dependent on both Casp9 and Casp3 is physiologically required for PCD in the developing brain.

Caspase 9– and Caspase 3–Independent Apoptotic Pathway

The requirement for Casp9 in apoptosis is cell type– and stimulus-specific, indicating the existence of multiple apoptotic pathways. Although *Casp9*$^{-/-}$ ES cells were resistant to a broad range of apoptotic stimuli, Casp9 deficiency did not protect other cell types from PCD induced by the same inducers. For example, unlike ES cells, *Casp9*$^{-/-}$ thymocytes and splenocytes underwent PCD in response to UV irradiation. *Casp3*$^{-/-}$ thymocytes and splenocytes are also sensitive to UV-induced cell

death. Thus, it is likely that an apoptotic pathway independent of both Casp9 and Casp3 exists in vivo.

Caspase 9–Independent and Caspase 3–Dependent Apoptotic Pathway

The existence of an apoptotic pathway independent of Casp9 but dependent on Casp3 is suggested by the response of activated T cells to α-CD95 and α-CD3ε. Casp3 deficiency has previously been shown to protect activated splenocytes from α-CD95– and α-CD3–induced apoptosis (Woo et al., 1998). However, Casp9 deficiency did not protect activated T cells from apoptosis induced by α-CD95 or α-CD3 and did not prevent Casp3 activation in response to these stimuli in vivo. These data strongly support the existence of a Casp9–independent, Casp3–dependent apoptotic pathway. Caspases with large prodomains containing CARDS, such as Casp4 and -8, have been shown to associate with Apaf1 (Hu et al., 1998). Thus, these caspases are possible candidates for the activation of this apoptotic pathway.

Caspase 9–Dependent and Caspase 3–Independent Apoptotic Pathway

Casp3$^{-/-}$ thymocytes have been shown to be sensitive to all apoptotic stimuli tested, including dexamethasone and γ irradiation (Kuida et al., 1996; Woo et al., 1998). In contrast, *Casp9*$^{-/-}$ thymocytes were resistant to PCD induced by dexamethasone or γ irradiation, implying that in thymocytes these stimuli trigger the activation of an apoptotic pathway that is Casp3–independent but Casp9–dependent. Of importance is the finding that γ irradiation preferentially activates this apoptotic pathway, since *Casp9*$^{-/-}$, but not *Casp3*$^{-/-}$, thymocytes, splenocytes, and ES cells were resistant to this apoptotic signal.

Coexistence of Parallel Apoptotic Pathways in Mammalian Cells: Implications for Drug Design

Our results lead us to propose that several apoptotic pathways coexist in mammalian cells that are preferentially activated in a cell type– and stimulus-specific manner. In considering drug therapy, the question as to whether a given apoptotic stimulus might trigger more than one apoptotic pathway is of great importance. Our findings support the possible costimulation in some cells of more than one apoptotic pathway in response to a single stimulus. For example, the Casp9–dependent and Casp3–independent apoptotic pathway is preferentially triggered in thymocytes in response to dexamethasone. However, the fact that Casp3 is still processed in dexamethasone-treated *Casp9*$^{-/-}$ thymocytes suggests that dexamethasone also activates a Casp9–independent and Casp3–dependent apoptotic pathway in these cells. The role of these coexisting pathways in normal development is under investigation in *Casp9*$^{-/-}$;*Casp3*$^{-/-}$ double mutant mice.

In conclusion, our results demonstrate that the requirement for Casp9 in apoptosis is cell type– and stimulus-specific. We have confirmed the existence in vivo of an apoptotic pathway dependent on both Casp9 and Casp3 and shown that this pathway is of particular importance in the developing brain. Given the critical role that Casp9 plays in the survival of neural progenitors within the embryonic forebrain and cortex, it will be interesting to determine whether Casp9 is involved in controlling postnatal neuronal survival in these sites following injury.

This work has also identified at least three novel physiological apoptotic pathways: one solely dependent on Casp9, another solely dependent on Casp3, and one independent of both these caspases. The existence of multiple pathways of apoptosis in mammalian cells has probably evolved to permit maximum flexibility in controlling cell fate. The understanding of these different apoptotic pathways and the design of drugs that specifically inhibit or stimulate them will assist in the treatment of the many diseases related to defects in apoptosis.

Experimental Procedures

Cells

E14 K embryonic stem cells from 129/Ola mice were maintained on a layer of mitomycin C–treated embryonic fibroblasts in ES cell medium, which was Dulbecco's modified Eagle's culture medium (DMEM), supplemented with leukemia inhibitory factor, 15% fetal calf serum (FCS), L-glutamine, and β-mercaptoethanol.

Generation of *Caspase 9*$^{-/-}$ Mutant Mice

A 129/J mouse genomic library was screened with a 400 bp mouse *Casp9* cDNA probe. Two phage carrying overlapping genomic clones encompassing *Casp9* were isolated. A targeting vector was designed to replace three *Casp9* coding exons, including the exon encoding the active site of Casp9 with the PGK*neo* resistance expression cassette. This strategy introduced stop codons into all three reading frames. The targeting vector (20 μg) was linearized with HpaI and electroporated into E14 K ES cells (5×10^6) (Bio-Rad Gene Pulser, 0.34 kV, 0.25 mF).

Electroporated cells were cultured in the presence of 300 μg/ml of G418 (Sigma) for 10 days. Homologous recombinants were identified by PCR according to standard procedures. An external primer (5′-GTA TGC TAT ACG AAG TTA TTA GTC C-3′) specific for the *Casp9* gene upstream of the targeting construct and a *neo* primer (5′-CTT ATG TAT TCC CGA GCC CGT GGT A-3′) specific for the neomycin resistance gene cassette were used in the PCR analysis. Colonies deemed positive by PCR were genotyped by Southern blotting using standard procedures. SpeI-digested DNA was hybridized to random hexamer ^{32}P-dCTP–labeled flanking probes (Amersham). Two correctly targeted colonies were identified.

Chimeric mice were generated by microinjection of *Casp9*$^{+/-}$ ES cells into E3.5 C57BL6/J blastocysts, which were transferred to CD1 pseudopregnant foster mothers. Chimeric males were mated with C57BL6/J females (Jackson Laboratories). Germline transmission of the mutant allele was verified by PCR and Southern blot analysis of tail DNA from F1 offspring with agouti coat color. Two targeted ES colonies successfully contributed to the germ line. F2 offspring from heterozygous intercrosses were genotyped by PCR and Southern blotting. The mutant phenotype was analyzed in 129/C57BL/6 and 129/CD1 genetic backgrounds; no significant differences were observed.

Generation of *Caspase 9*$^{-/-}$ ES Cells and *Caspase 9*$^{-/-}$; *Rag2*$^{-/-}$ Chimeras

Independent *Casp9*$^{-/-}$ ES clones were generated from the two *Casp9*$^{+/-}$ ES clones by culture in an increased concentration of G418 (2 mg/ml). Colonies that were resistant to this dose of G418 were analyzed for homologous recombination of the second allele by PCR using primers specific for the deleted portion of the *Casp9* gene (5′-CTT TGT CCC TCC TGT TGT GTC TTC A−3′ and 5′-CAG AGC GAG AAT GAA GGG GAA ACA-3′). Colonies that were homozygous by PCR for the *Casp9* mutation were expanded and their

genotypes confirmed by Southern blot analysis. Two homozygous *Casp9*$^{-/-}$ ES clones, as well as a parental clone, were injected into 3.5-day *Rag2*$^{-/-}$ blastocysts and transferred to pseudopregnant foster mothers. *Casp9*$^{-/-}$*; Rag2*$^{-/-}$ and *Casp9*$^{+/-}$*; Rag2*$^{-/-}$ offspring chimeric mice were used to study thymocyte and splenocyte apoptosis in adult mice.

RNA Analysis

Two micrograms of poly (A)$^+$ RNA from E7, E11, E15, and E17 mouse embryos and different adult mouse tissues were analyzed by Northern blot (Clontech). Standard procedures were used to hybridize blots to the same ^{32}P-dCTP–labeled *Casp9* cDNA probe used for genomic library screening.

Histological Analysis

Embryos at stages E10.5, E12.5, and E15.5, as well as brains from postnatal day 1 mice, were isolated in ice-cold PBS, fixed overnight in 4% paraformaldehyde at 4°C, dehydrated, and embedded in paraffin. Five micrometers horizontal or coronal sections were cut and stained with thionin.

BrdU Labeling

BrdU (100 μg/gram of body weight) was injected intraperitoneally into pregnant females at E12.5 and E15.5. The females were sacrificed 1 hr after injection, and the embryos were fixed in 4% paraformaldehyde at 4°C overnight and processed for immunohistochemistry as described previously (Hakem et al., 1996). The sections were incubated with an α-BrdU MAb (Boehringer Mannheim) at a 1:10 dilution. Staining was performed according to the protocol described previously (Mishina et al., 1995).

TUNEL Assay

For the TUNEL assay, an "in situ cell death detection kit " was used (Boehringer Mannheim). Briefly, paraffin-embedded sections were dewaxed and rehydrated in PBS according to standard protocols. Sections were then incubated with proteinase K (20 μg/ml in 10 mM Tris-HCl [pH 7.5]) for 15 min at 37°C. The TUNEL reaction mixture (containing DNA polymerase as well as terminal deoxynucleotidyl transferase [TdT] and labeled nucleotides) was applied to the sections in a humidified chamber and incubated for 60 min at 37°C. Sections were then washed in PBS, mounted in "antifade" medium, and analyzed under a fluorescence microscope.

Induction of Apoptosis in ES Cells

Cells (1×10^5) of one *Casp9*$^{+/-}$ and two *Casp9*$^{-/-}$ ES cell clones were plated on 1% gelatinized plates (24-well plates; Costar) in ES cell medium. At 12 hr after the initial plating at 37°C, the following cell death stimuli were administered: UV irradiation at 40 or 80 mJ/cm^2 using DNA-Stratalinker (Stratagene); γ irradiation at 300 or 600 rads (Gammacell 40 Exactor); sorbitol at 0.1 M or 0.4 M; etoposide at 100 μM; adriamycin at 0.3 or 3 μg/ml; anisomycin at 0.05 mM; or cisplatinum at 10 μg/ml (Sigma). Cells were harvested 16, 24, or 48 hr after the induction of cell death, and apoptosis was determined by FACS analysis (FACSCalibur, Becton Dickinson, San Jose, CA) using Annexin V-FITC and propidium iodide (PI) according to the manufacturer's instructions (RandD Systems). CellQuest software (BD) was used to analyze 10,000 gated events. Viable cells were identified by their ability to exclude Annexin V and PI. For visualization of chromatin condensation, cells (1×10^5) were fixed in 4% paraformaldehyde, and DNA was stained with DAPI (1 μg/ml; Sigma). The condensation state of the chromatin was visualized using a fluorescence microscope (Leica). Casp3 and Casp3–like activities were assayed using the fluorogenic caspase substrate AcDEVD-AMC according to the manufacturer's instructions (Pharmingen).

Analysis of PCD by Electron Microscopy

Pelleted cells were resuspended in cold 3% glutaraldehyde in 0.1 M sodium cacodylate buffer. After 48 hr in fixative, the cells were rinsed in cacodylate buffer and postfixed in 1% aqueous osmium tetroxide for 1 hr. Samples were rinsed and dehydrated through a series of graded ethanol solutions prior to embedding in epoxy resin. Ultrathin sections were contrast-enhanced with uranyl acetate and lead citrate and examined using a Phillips CM120 transmission electron microscope.

Apoptosis in MEFs

MEFs derived from E15.5 embryos were prepared according to standard procedures. All cultures were maintained in DMEM (GIBCO) supplemented with 5% FCS and 1% penicillin G/streptomycin sulfate (Sigma). Cells (1×10^5) from one *Casp9*$^{+/-}$ and two *Casp9*$^{-/-}$ MEF cultures were plated on 24-well plates in MEF medium. At 12 hr after the initial plating at 37°C, the following cell death stimuli were administered: UV irradiation at 40 or 80 mJ/cm^2 using DNA-Stratalinker; γ irradiation at 300 or 600 rads; etoposide at 100 μM; or adriamycin at 0.3 or 3 μg/ml. Cells were harvested 24 or 48 hr after the induction of cell death, stained with Annexin V and PI, and analyzed by flow cytometry.

Apoptosis was also investigated in MEFs transiently transfected with the *Green Fluorescein Protein* expression vector (2 μg), alone or in combination with *TNF-R1* expression vector (2 μg), using LIPOFECTAMINE PLUS reagents (GIBCO). Cells were trypsinized 24 hr after transfection, supernatants were collected, and cell viability (% of fluorescent cells) was determined by FACS analysis.

Transformation of MEFs with *E1A* and *ras* was performed as previously described (Woo et al., 1998). Transformed cells ($3–4 \times 10^6$) were plated in 10 cm plates (2 plates per treatment). After 8 hr, cells were washed twice with PBS and treated with the indicated amounts of adriamycin or mTNF-α (Boehringer Mannheim) in DMEM containing 10% FCS. Adherent and nonadherent cells were pooled after treatment, and viability was assayed by trypan blue exclusion. To analyze chromatin changes in transformed wild-type and *Casp9*$^{-/-}$ MEFs, cells were either left untreated or treated with adriamycin (0.2 μg/ml) or mTNF-α (50 ng/ml) for 24 hr. Attached, untreated (alive), and detached (dead) cells were stained with DAPI.

Apoptosis in Thymocytes

Single cell suspensions of thymocytes were prepared and washed twice in RPMI containing 10% FCS (complete medium, CM). Thymocytes were resuspended at 5×10^6/ml in CM and plated in a final volume of 1 ml in 24-well flat bottom tissue culture plates. The following cell death stimuli were administered: dexamethasone (Sigma) at 0.1 μM or 1 μM; γ irradiation at 300 or 600 rads; etoposide at 100 μM; α-CD95 (Jo2, Pharmingen) at 0.1 or 1 μg/ml; UV irradiation at 40 or 80 mJ/cm^2; sorbitol at 0.1 mM or 0.4 M; or heat shock at 43°C for 1 hr. Treated and untreated thymocytes were cultured for 24 hr at 37°C in 5% CO_2, followed by harvesting, staining with Annexin V and PI, and FACS analysis. DAPI staining was also performed to assess chromatin condensation.

Measurement of Mitochondrial Membrane Potential and Apoptotic Cells by Flow Cytometry

Thymocyte death was induced with 1 μM dexamethasone, and cells were harvested 30 min prior to the experimental endpoint (3, 6, 18, or 24 hr). Harvested cells were incubated in CM containing 40 nM 1,1′,3,3′,3′-hexamethylindodicarbocyanine iodide [$DiIC_1(5)$] (Molecular Probes) for 30 min at 37°C in 5% CO_2. Cells were subsequently washed by centrifugation (800 g, 5 min), stained with Annexin V and PI, and analyzed by flow cytometry. Loss of $\Delta\psi m$ was visualized as a reduction in the signal in FL4 as cells underwent apoptosis. Comparison of identical samples double-stained with Annexin V and PI or triple-stained with Annexin V, PI, and $DiIC_1(5)$ showed that the addition of $DiIC_1(5)$ had no adverse effects on cell viability as assessed by PS residue exposure or $\Delta\psi m$.

Apoptosis of Activated Splenocytes

Splenocytes from wild-type and *Casp9*$^{-/-}$ mice were isolated and cultured with plate-bound α-CD3ε (10 μg/ml) for 24 hr, followed by culture in media containing murine recombinant IL-2 (30 μg/ml; Genzyme) for 4 days. The activated lymphocytes were treated with either plate-bound α-CD3ε (1 or 5 μg/ml) or α-CD95 (0.1 or 1 μg/ml) for 24 or 48 hr. Treated cells were then analyzed for apoptosis by Annexin V and PI staining as well as by DAPI staining.

Cytochrome c Release from Mitochondria

Casp9$^{-/-}$ and *Casp9*$^{+/-}$ ES cells (10×10^6) plated on 10 cm cell culture dishes were either left untreated or subjected to UV irradiation (80 mJ/cm^2). Six hours after irradiation, cells were harvested by centrifugation at 600 × g for 10 min. Cytosolic fractions (S-100) were prepared from these cells as previously described (Yang et al., 1997). Cell pellets were washed twice with cold PBS and resuspended in 5 vol of buffer A (20 mM HEPES-KOH [pH 7.5], 10 mM KCl, 1.5 mM $MgCl_2$, 1 mM Na EDTA, 1 mM Na EGTA, 1 mM dithiothreitol, and 0.1 mM phenylmethylsulfonyl fluoride) in the presence of 250 mM sucrose. The cells were homogenized with 25 strokes of a Teflon homogenizer, followed by two rounds of centifugation at 750 × g for 10 min at 4°C. The supernatants were then centrifuged at 10,000 × g for 15 min at 4°C. The resulting supernatants were further centrifuged at 100,000 × g for 1 hr at 4°C. The final supernatants were collected, aliquoted, and stored at −70°C. Cytochrome c was identified in the cytosolic fractions by Western blotting.

Western Blotting

Cells were lysed in 1% NP-40 lysis buffer (1% NP-40, 150 mM NaCl, 50 mM Tris-HCl [pH 8.0], 1 mM sodium vanadate) supplemented with protease inhibitor cocktail (0.1 mM PMSF, 2 μg/ml of leupeptin and apoprotein) for 15 min on ice. Lysates were centrifuged at 10,000 rpm for 5 min at 4°C, and protein concentration was estimated by the Pierce Protein Assay, using BSA as the standard. Thirty micrograms of total protein was loaded onto 10% or 14% SDS-PAGE, transferred onto nitrocellulose membranes, and incubated with the appropriate antibodies. Antibodies reactive to Casp3 (gift of R. Sekaly, Montreal), Casp2 and -7 (Santa Cruz), Casp8 and -9 (generated against Casp8 peptide SNKDDRRNKGKQMPC and Casp9 peptide SQGRTLDSDSEPDAVPYQEGPRPC), PARP (Boehringer Mannheim), Rb (G3-245, Pharmingen), cytochrome c (7H8.2C12, Pharmingen), or anti-β actin (Sigma) were used in this study. Western blot analysis was carried out according to standard procedures using ECL detection (Amersham).

Acknowledgments

This paper is dedicated to Shirley S.-W. Mak and all victims of breast cancer. We thank all of Amgen's groups for invaluable reagents; Raffick Sekaly for the α-Casp3 antibody and David Goeddel for the *TNF-R1* expression vector; Wen-Chen Yeh, Alex Grossman, Drew Wakeham, Sarosi Ildiko, and Denis Bouchard for helpful comments; and Mary Saunders for scientific editing. A. H. is supported by a grant from the Medical Research Council of Canada. M. S. S. is supported by a postdoctoral fellowship from the Spanish Ministry of Education and Human Frontiers Science Foundation. S. W. L. is a Kimmel Scholar. This work was supported by grant CA13106 from the National Cancer Institute, USA (S. W. L), and by the National Cancer Institute of Canada and Medical Research Council of Canada (T. W. M.).

Received June 12, 1998; revised July 7, 1998.

References

Bakhshi, A., Jensen, J.P., Goldman, P., Wright, J.J., McBride, O.W., Epstein, A.L., and Korsmeyer, S.J. (1985). Cloning the chromosomal breakpoint of t(14;18) human lymphomas: clustering around JH on chromosome 14 and near a transcriptional unit on 18. Cell *41*, 899–906.

Bergeron, L., Perez, G.I., Macdonald, G., Shi, L., Sun, Y., Jurisicova, A., Varmuza, S., Latham, K.E., Flaws, J.A., Salter, J.C., et al. (1998). Defects in regulation of apoptosis in caspase-2-deficient mice. Genes Dev. *12*, 1304–1314.

Bossy, W.E., Newmeyer, D.D., and Green, D.R. (1998). Mitochondrial cytochrome c release in apoptosis occurs upstream of DEVD-specific caspase activation and independently of mitochondrial transmembrane depolarization. EMBO J. *17*, 37–49.

Cheng, E.H., Kirsch, D.G., Clem, R.J., Ravi, R., Kastan, M.B., Bedi, A., Ueno, K., and Hardwick, J.M. (1997). Conversion of Bcl-2 to a Bax-like death effector by caspases. Science *278*, 1966–1968.

Clem, R.J., Cheng, E.H., Karp, C.L., Kirsch, D.G., Ueno, K., Takahashi, A., Kastan, M.B., Griffin, D.E., Earnshaw, W.C., Veliuona M.A., et al. (1998). Modulation of cell death by Bcl-XL through caspase interaction. Proc. Natl. Acad. Sci. USA *95*, 554–559.

Cohen, G.M. (1997). Caspases: the executioners of apoptosis. Biochem. J. *326*, 1–16.

Deckwerth, T.L., Elliott, J.L., Knudson, C.M., Johnson, E.M., Jr., Snider, W.D., and Korsmeyer, S.J. (1996). BAX is required for neuronal death after trophic factor deprivation and during development. Neuron *17*, 401–411.

Deveraux, Q.L., Roy, N., Stennicke, H.R., Van Arsdale, T., Zhou, Q., Srinivasula, S.M., Alnemri, E.S., Salvesen, G.S., and Reed, J.C. (1998). IAPs block apoptotic events induced by caspase-8 and cytochrome c by direct inhibition of distinct caspases. EMBO J. *17*, 2215–2223.

Donehower, L.A. (1996). The p53-deficient mouse: a model for basic and applied cancer studies. Semin. Cancer Biol. *7*, 269–278.

Duan, H., Orth, K., Chinnaiyan, A.M., Poirier, G.G., Froelich, C.J., He, W.W., and Dixit, V.M. (1996). ICE-LAP6, a novel member of the ICE/Ced-3 gene family, is activated by the cytotoxic T cell protease granzyme B. J. Biol. Chem. *271*, 16720–16724.

Green, D.R., and Martin, S.J. (1995). The killer and the executioner: how apoptosis controls malignancy. Curr. Opin. Immunol. *7*, 694–703.

Hakem, R., de la Pompa, J.L., Sirard, C., Mo, R., Woo, M., Hakem, A., Wakeham, A., Potter, J., Reitmair, A., Billia, F., et al. (1996). The tumor suppressor gene Brca1 is required for embryonic cellular proliferation in the mouse. Cell *85*, 1009–1023.

Hengartner, M.O. (1996). Programmed cell death in invertebrates. Curr. Opin. Genet. Dev. *6*, 34–38.

Hu, Y., Benedict, M.A., Wu, D., Inohara, N., and Nunez, G. (1998). Bcl-XL interacts with Apaf-1 and inhibits Apaf-1-dependent caspase-9 activation. Proc. Natl. Acad. Sci. USA *95*, 4386–4391.

Kharbanda, S., Pandey, P., Schofield, L., Israels, S., Roncinske, R., Yoshida, K., Bharti, A., Yuan, Z.M., Saxena, S., Weichselbaum, R., et al. (1997). Role for Bcl-xL as an inhibitor of cytosolic cytochrome C accumulation in DNA damage-induced apoptosis. Proc. Natl. Acad. Sci. USA *94*, 6939–6942.

Kluck, R.M., Bossy, W.E., Green, D.R., and Newmeyer, D.D (1997). The release of cytochrome c from mitochondria: a primary site for Bcl-2 regulation of apoptosis. Science *275*, 1132–1136.

Knudson, C.M., Tung, K.S., Tourtellotte, W.G., Brown, G.A., and Korsmeyer, S.J. (1995). Bax-deficient mice with lymphoid hyperplasia and male germ cell death. Science *270*, 96–99.

Kuida, K., Lippke, J.A., Ku, G., Harding, M.W., Livingston, D.J., Su, M.S.-S., and Flavell, R.A. (1995). Altered cytokine export and apoptosis in mice deficient in interleukin-1 beta converting enzyme. Science *267*, 2000–2003.

Kuida, K., Zheng, T.S., Na, S., Kuan, C.K., Yang, D., Karasuyama, H., Rakic, P., and Flavell, R.A. (1996). Decreased apoptosis in the brain and premature lethality in CPP32-deficient mice. Nature *384*, 368–372.

Li, F., Srinivasan, A., Wang, Y., Armstrong, R.C., Tomaselli, K.J., and Fritz, L.C. (1997a). Cell-specific induction of apoptosis by microinjection of cytochrome c. Bcl-xL has activity independent of cytochrome c release. J. Biol. Chem. *272*, 30299–30305.

Li, P., Nijhawan, D., Budihardjo, I., Srinivasula, S.M., Ahmad, M., Alnemri, E.S., and Wang, X., (1997b). Cytochrome c and dATP-dependent formation of Apaf-1/Caspase-9 complex initiates an apoptotic protease cascade. Cell *91*, 479–489.

Liston, P., Roy, N., Tamai, K., Lefebvre, C., Baird, S., Cherton-Horvat, G., Farahani, R., McLean, M., Ikeda, J.E., MacKenzie, A., et al. (1996). Suppression of apoptosis in mammalian cells by NAIP and a related family of IAP genes. Nature *379*, 349–353.

Lowe, S.W., Schmitt, E.M., Smith, S.W., Osborne, B.A., and Jacks, T. (1993). p53 is required for radiation-induced apoptosis in mouse thymocytes. Nature *362*, 847–849.

Mignotte, B., and Vayssiere, J.L. (1998). Mitochondria and apoptosis. Eur. J. Biochem. *252*, 1–15.

Mishina, Y., Suzuki, A., Ueno, N., and Behringer, R.R. (1995). Bmpr

encodes a type I bone morphogenetic protein receptor that is essential for gastrulation during mouse embryogenesis. Genes Dev. *9*, 3027–3037.

Motoyama, N., Wang, F., Roth, K.A., Sawa, H., Nakayama, K., Nakayama, K., Negishi, I., Senju, S., Zhang, Q., Fujii, S., et al. (1995). Massive cell death of immature hematopoietic cells and neurons in Bcl-x-deficient mice. Science *267*, 1506–1510.

Nagata, S. (1997). Apoptosis by death factor. Cell *88*, 355–365.

Pan, G., O'Rourke, K., and Dixit, V.M. (1998). Caspase-9, Bcl-XL, and Apaf-1 form a ternary complex. J. Biol. Chem. *273*, 5841–5845.

Reed, J.C. (1994). Bcl-2 and the regulation of programmed cell death. J. Cell. Biol. *124*, 1–6.

Roy, N., Deveraux, Q.L., Takahashi, R., Salvesen, G.S., and Reed, J.C. (1997). The c-IAP-1 and c-IAP-2 proteins are direct inhibitors of specific caspases. EMBO J. *16*, 6914–6925.

Salvesen, G.S., and Dixit, V.M. (1997). Caspases: intracellular signaling by proteolysis. Cell *91*, 443–446.

Sentman, C.L., Shutter, J.R., Hockenbery, D., Kanagawa, O., and Korsmeyer, S.J. (1991). bcl-2 inhibits multiple forms of apoptosis but not negative selection in thymocytes. Cell *67*, 879–888.

Srinivasula, S.M., Fernandes-Alnemri, T., Zangrilli, J., Robertson, N., Armstrong, R.C., Wang, L., Trapani, J.A., Tomaselli, K.J., Litwack, G., and Alnemri, E.S. (1996). The Ced-3/interleukin 1beta converting enzyme-like homolog Mch6 and the lamin-cleaving enzyme Mch2alpha are substrates for the apoptotic mediator CPP32. J. Biol. Chem. *271*, 27099–27106.

Steller, H. (1995). Mechanisms and genes of cellular suicide. Science *267*, 1445–1449.

Thompson, C.B. (1995). Apoptosis in the pathogenesis and treatment of disease. Science *267*, 1456–1462.

Tsujimoto, Y., Gorham, J., Cossman, J., Jaffe, E., and Croce, C.M. (1985). The t(14;18) chromosome translocations involved in B-cell neoplasms result from mistakes in VDJ joining. Science *229*, 1390–1393.

Wang, S., Miura, M., Jung, Y.-K., Zhu, H., Li, E., and Yuan, J. (1998). Murine caspase-11, an ICE-interacting protease, is essential for the activation of ICE. Cell *92*, 501–509.

White, E. (1993). Death-defying acts: a meeting review on apoptosis. Genes Dev. *7*, 2277–2284.

Woo, M., Hakem, R., Soengas, M.S., Duncan, G.S., Shahinian, A., Kagi, D., Hakem, A., McCurrach, M., Khoo, W., Kaufman, S.A., et al. (1998). Essential contribution of caspase 3/CPP32 to apoptosis and its associated nuclear changes. Genes Dev. *12*, 806–819.

Yang, J., Liu, X., Bhalla, K., Kim, C.N., Ibrado, A.M., Cai, J., Peng, T.I., Jones, D.P., and Wang, X. (1997). Prevention of apoptosis by Bcl-2: release of cytochrome c from mitochondria blocked. Science *275*, 1129–1132.

Zhivotovsky, B., Orrenius, S., Brustugun, O.T., and Doskeland, S.O. (1998). Injected cytochrome c induces apoptosis. Nature *391*, 449–450.

Zou, H., Henzel, W.J., Liu, X., Lutschg, A., and Wang, X. (1997). Apaf-1, a human protein homologous to C. elegans CED-4, participates in cytochrome c-dependent activation of caspase-3. Cell *90*, 405–413.